INTERNATIONAL BACCULEARATE – DIPLOMA PROGRAM

Subject: Group 4 (Physics)

Anusha Fatima Alam

Topic: Investigating the Wall Effect on a Ball Bearing

Research Question: How does the relative radii of a ball bearing affect the relative drag force experienced within a Newtonian fluid?

Session: May 2022

Word Count: 3999

Table of Contents

I. INTRODUCTION

Fluid dynamics is an integral part of fluid mechanics that has vast applications within the field of aerodynamics and industrial engineering. A concept important to these fields is the drag coefficient, which is a parameter utilized in the designing process of industrial equipment. Often objects of different shapes and sizes are submerged inside a single channel which experience varying levels of drag force with respect to the proximity with the wall, namely called “The Wall Effect”, a phenomenon where a finite boundary exerts a retarding force on the terminal velocity of an object in a viscous medium (Ataíde). This occurs typically inside a bounded medium (see figure 1.1 and 1.2) where a sphere is settling along the axis of cylindrical tubes.

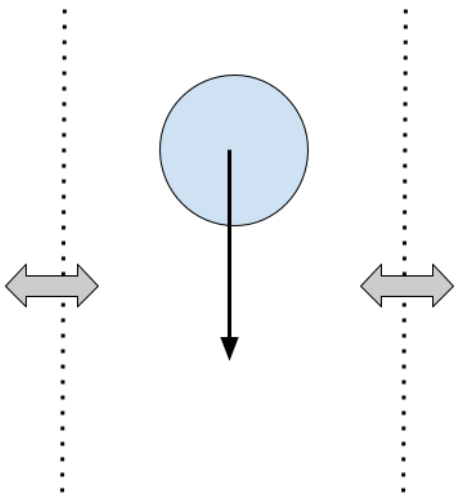

Figure 1.1 A Ball bearing falling through an unbounded medium (Candidate, 2021)

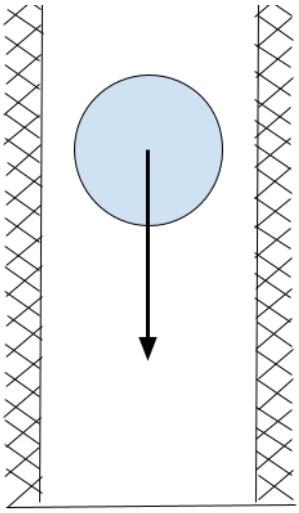

Figure 1.2 A Ball bearing falling inside a bounded medium with fixed boundaries (Candidate, 2021)

The wall effect does not only impact the hydrodynamic behavior of fluids but also affects the heat transfer performance of the overall system (Samantaray). In a real-life context, evidence of objects being submerged within channels is prominent in the food industry where fruits are vegetables are dried inside

cylindrical tubes, or particles present inside meshed solids or bioengineering devices that travel through the blood vessels. Although many industrial processes handle systems with multi-particles travelling through a single channel, the hydrodynamics of a single particle is sufficient to provide information about settling behaviors inside multi-particle systems. Having interest in industrial engineering and food industry, the chosen topic of exploration is the wall effect on the flow of objects submersed in a single tube.

This essay will explore the impact of the relative radius of the bounded medium (the ratio of the radius of ball bearing to the radius of tube) on the relative drag.

II. RESEARCH QUESTION

How does the relative radii of a ball bearing affect the relative drag force experienced within a Newtonian fluid?

III. APPROACH

An experimental & theoretical approach is taken. The terminal velocity will be measured by tracking the motion of the ball bearing at different relative radii and will be used to process the relative drag.

IV. BACKGROUND INFORMATION

a. Determining the drag force acting on a spherical body

For a spherical object falling vertically through a fluid medium, it experiences an upward drag and buoyancy force and a downward gravitational force (which is equivalent to $F_g = -mg$), assuming no rotational forces and/or lateral forces of the container are acting. As soon as the sphere reaches translational equilibrium (see figure 2.1), it will travel at a constant terminal velocity, v.

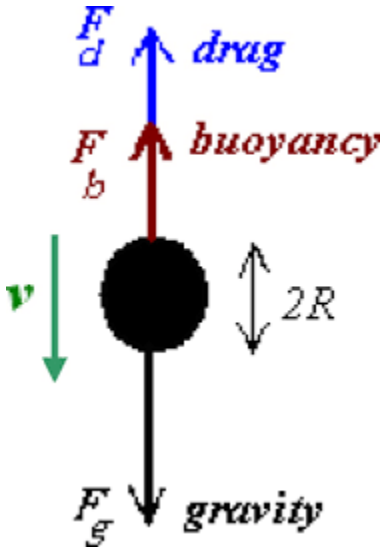

Figure 2.1 Free-Body Diagram of a sphere falling through a fluid medium (Ahmed)

For an object in translational equilibrium:

$$F_{Upward} = F_{Downward} \quad (1)$$

$$F_{Weight} = F_{Drag} + F_{Buoyancy} \quad (2)$$

Equation 2 can be rearranged as:

$$F_{Drag} = F_{Weight} - F_{Buoyancy} \quad (3)$$

The buoyant force acting on the sphere submerged inside a fluid is equivalent to the weight of the liquid displaced ($F_B = m_{liquid}g$). $m = pV$, where m is mass, V is volume and p is density. Since the volume of displaced by the submerged object is equivalent to the volume of the spherical body, both will be denoted by V.

$$\therefore F_{Drag} = m_{sphere}g - p_{fluid}Vg \quad (4)$$

where g is acceleration due to gravity.

Substituting $m_{sphere} = p_{sphere}V$

$$F_{Drag} = p_{sphere}Vg - p_{fluid}Vg = Vg(p_{sphere} - p_{fluid}) \quad (5)$$

Since $V = \frac{4}{3}\pi {r_0}^3$ for a spherical object with a radius r_0:

$$\boldsymbol{F_{Drag} = \frac{4}{3}\pi {r_0}^3 g(p_{sphere} - p_{fluid})}. \quad (6)$$

b. Understandings of Fluid Mechanics

Types of Fluid Flow:

- Laminar Flow – Laminar flow describes motion of particles in infinitesimal straight lines parallel to each other, where viscous forces predominate inertial forces (Ramsey). The wall effect is experienced within laminar flow (a constraint of Stokes law).
- Turbulent Flow – Turbulent flow describes a flow where the fluid undergoes irregular fluctuations characterized by eddies, where the inertial forces predominate the viscous forces (Ramsey).

There are two types of forces acting on fluids:

- Inertial Forces arise due to the momentum of a fluid.
- Viscous forces arise due to the friction between layers of the fluid and the resistance of a fluid to flow. The friction between fluid particles also produces shear stress which causes shear deformation of fluids.

c. Stokes Law

When a spherical object is falling through a viscous fluid, the lower hemisphere is pushed, and the upper hemisphere is pulled by the viscous forces of the fluid which creates a net shearing force between the solid sphere and the fluid as shown in figure 2.3.

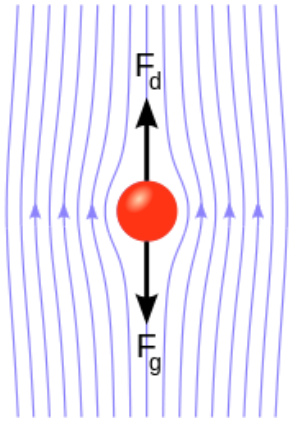

Figure 2.1 *Ideal flow around a sphere ("Deriving Stokes' Law in a Simple Way.")*

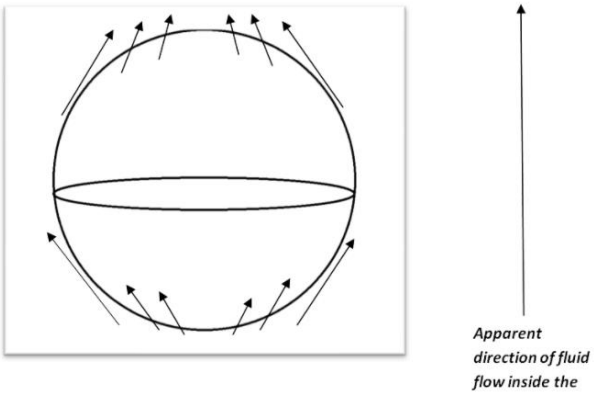

Figure 2.3 *Net Shearing force acting on a Spherical Body ("Proof of Stokes Law of Viscosity Using Reynolds Law.")*

According to the Stokes law (***Refer to Appendix A)***, the frictional force acting on the interface of a sphere falling vertically inside a viscous medium is proportional to the viscosity of the medium, the radius of the sphere and the velocity of the sphere, expressed by:

$$\boldsymbol{F_{Drag} = 6\pi r_0 \eta v} \qquad (7)$$

where r_0 is the radius of the spherical object, η is the viscosity of the fluid and v is the velocity of the sphere which *is the definition of stokes law.*

Equating equation 6 with equation 7:

$$6\pi r_0 \eta v = \frac{4}{3}\pi {r_0}^3 g\left(p_{sphere} - p_{fluid}\right) \qquad (8)$$

$$\therefore 6\eta v = \frac{4}{3} {r_0}^2 g\left(p_{sphere} - p_{fluid}\right) \quad (9)$$

Since the spherical body has reached translational equilibrium, it must be travelling at a constant and maximum terminal velocity. Therefore v can be replaced by v_t which is the terminal velocity (ms^{-1}) of the object.

This can be rearranged to make, η, viscosity subject of the formula:

$$\boldsymbol{\eta = \frac{2{r_0}^2 g}{9v_t}\left(p_{sphere} - p_{fluid}\right)} \quad (10)$$

The relative drag is equivalent to the ratio of the viscosity of the fluid in the bounded medium and unbounded medium respectively.

d. Navier-Stokes Partial Differential Equation

Navier-stokes equation describe the relation between “the pressure, temperature and density of a moving incompressible fluid” (Hall) and is extremely useful in modelling the flow around objects and minimizing drag around objects. According to Navier-Stokes equation:

$$\underbrace{\rho\left(\frac{\partial u}{\partial t} + u\frac{\partial u}{\partial x} + v\frac{\partial u}{\partial y}\right)}_{\text{Inertia Term}} = \underbrace{\rho X}_{\text{Body Force Term}} - \underbrace{\frac{\partial p}{\partial x}}_{\text{Pressure Term}} + \underbrace{\eta\left(\frac{\partial^2 u}{\partial x^2} + \frac{\partial^2 u}{\partial y^2}\right)}_{\text{Viscous Term}} \quad (11)$$

where y is velocity in y-direction, u is velocity in x-direction, X is acceleration in x-direction, η is fluid viscosity and ρ is pressure.

i. Laminar Flow between Parallel Surfaces

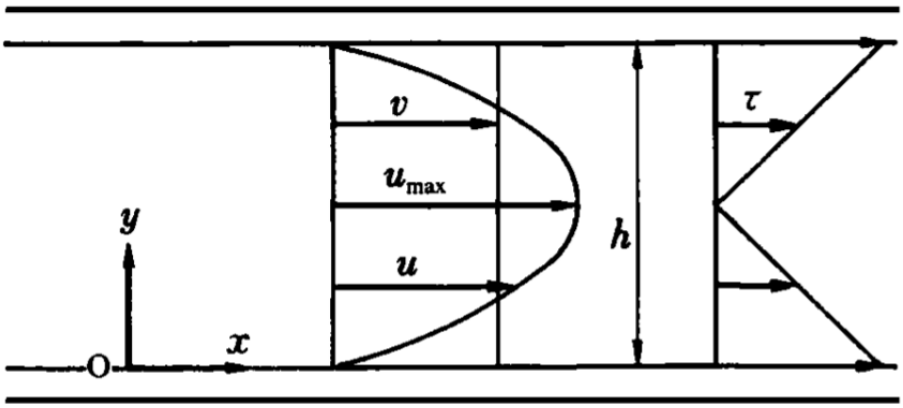

Figure 2.5 *Annotated Diagram of variables for Laminar Flow between parallel surfaces (Nakayama, 89)*

Laminar flow between parallel surfaces is taken into consideration because flow inside a circular tube can be assumed to act like parallel plates with axial symmetry. The velocity distribution for laminar flow inside parallel surfaces (see figure 2.5) can be simplified using the Navier-Stokes equation under the following assumptions:

- $\frac{\partial u}{\partial t} = 0$ *(The flow is steady;* u *doesn't change with respect to time)*
- $\rho X = 0$ *(There is no body force, zero acceleration)*
- $v = 0$ *(no velocity in the y-direction)*
- $\frac{\partial u}{\partial x} = 0$ & $\frac{\partial^2 u}{\partial x^2} = 0$ *(The flow is uniform;* u *does not change with respect to the position)*

$$\therefore \eta \frac{\partial^2 u}{\partial y^2} = \frac{dp}{dx} \qquad (12)$$

Integrating the equation above **twice** with respect to y (Nakayama, 90)

$$2\eta u = \frac{dp}{dx}y^2 + c_1 y + c_2 \qquad (13)$$

Rearranging the equation above to make u the subject:

$$u = \frac{1}{2\eta}\frac{dp}{dx}y^2 + c_1 y + c_2 \qquad (14)$$

In fluid dynamics, the no-slip boundary condition (for viscous fluids inside a solid boundary) assumes that velocity is zero relative to the boundary. The arbitrary constants ($c_1\ and\ c_2$) in equation 14 can be determined using the no slip boundary condition (where $u = 0,\ y = 0\ and\ y = h$) to produce a definite integral. $y = 0\ and\ y = h$ corresponds to the upper and lower boundaries of the parallel plates.

At $u = 0\ and\ \ y = 0$

$$\frac{1}{2\eta}\frac{dp}{dx}(0)^2 + c_1(0) + c_2 = 0 \qquad (15)$$

Therefore $c_2 = 0$

At $u = 0\ and\ \ y = h$, where h is the distance between the plates.

$$\frac{1}{2\eta}\frac{dp}{dx}(h)^2 + c_1(h) = 0 \qquad (16)$$

Therefore $c_1 = -\frac{1}{2\eta}\left(\frac{dp}{dx}\right)h$.

Substituting $c_1\ and\ c_2$ and factoring $\frac{1}{2\eta}\left(\frac{dp}{dx}\right)$:

$$u = \left(\frac{1}{2\eta}\right)\left(\frac{dp}{dx}\right)y(y-h) \qquad (17)$$

It forms a parabolic velocity distribution.

e. Theoretical Determination

At a very low velocity, for a small particle the drag force is approximately proportional to the velocity, $F_{Drag} = -bv$, where b is the drag coefficient and the negative sign implies that the drag force acts opposite to the velocity (Nave). For sphere (of radius r_0) falling through a viscous fluid inside a tube (of radius R), it experiences a drag force of $F_{Drag} = 6\pi r_0 \eta v$, however the drag coefficient $b > 6\pi r_0 \eta$ because of the parabolic nature of the velocity profile as described in equation 17. This means that there will be a greater wall shear stress and therefore a greater friction force.

The ball bearing is static, and the fluid is flowing with respect to the sphere during the fall. Since the sphere reaches its terminal velocity, it can be assumed that the velocity of fluid above the hemisphere is the same as the velocity of the fluid below the hemisphere. Hence the centerline velocity, v, would remain constant throughout.

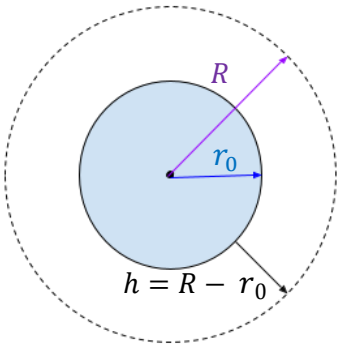

Figure 2.6 *Annotated Diagram of a Ball Bearing on Google Drawing (Candidate, 2021)*

The velocity profile for laminar flow inside parallel plates is $u = \left(\frac{1}{2\eta}\right)\left(\frac{dp}{dx}\right) y(y-h)$. Because $\frac{dp}{dx}$ (change in pressure with respect to position x) is unknown, $\left(\frac{1}{2\eta}\right)\left(\frac{dp}{dx}\right)$ can be substituted by an unknown variable a which is a scale factor of function u.

Therefore $u = ay(y - h)$. The zeroes of this velocity profile lie at $y = 0$ and $y = R - r$ (see figure 2.6 above) where r is the radius of the ball (which lies between $0 < r < r_0$). Therefore letting $h = R - r$:

$$u = ay(y - (R - r)) \qquad (18)$$

First, a can be computed by analyzing the parabolic nature of the velocity distribution described by equation 30. Graphing equation 30 gives the following graph:

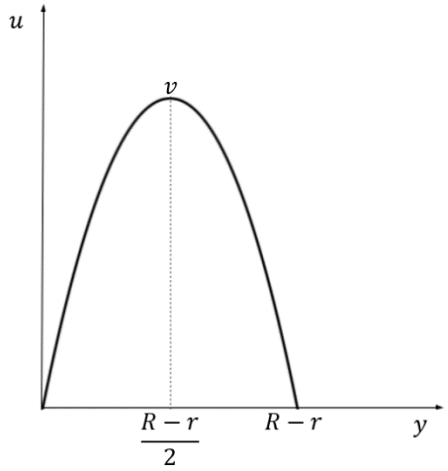

Figure 2.7 *Parabolic Velocity Profile on Google Drawing (Candidate, 2021)*

Using the property of the graph 2.7 we can obtain a by substituting into equation 18.

$u = v$, where v is the maximum terminal velocity and $y = \frac{R-r}{2}$. This will help determine $\frac{du}{dy}$ and calculate the frictional drag and shear stress:

$$\therefore\ v = -a\frac{(R-r)^2}{4} \qquad (19)$$

$$\therefore\ a = -\left(\frac{1}{4\eta}\right)\left(\frac{dp}{dx}\right) = \frac{-4v}{(R-r)^2} \qquad (20)$$

where R is the radius of the circular tube.

Thus velocity profile u in terms of y equals

$$u = \frac{-4v}{(R-r)^2}y(y - (R - r)) \qquad (21)$$

Differentiating equation 21 with respect to y

$$\frac{du}{dy} = \frac{-4v}{(R-r)^2}(2y - (R - r)) \qquad (22)$$

At the sphere's surface where $y = R - r$,

$$\frac{du}{dy} = \frac{-4v}{(R-r)^2}\big(2(R-r) - (R-r)\big) = \frac{-4v}{(R-r)^2}\,(R-r) = \frac{-4v}{(R-r)} \qquad (23)$$

The shear stress τ_0 due to viscosity of the fluid inside the tube equals

$$\tau_0 = \eta \frac{du}{dy} \qquad (24)$$

Substituting $\frac{du}{dy}$ (equation 23)

$$\tau_0 = \eta \left(\frac{-4v}{(R-r)}\right) = \frac{-4\eta v}{(R-r)} \qquad (25)$$

The vector component of shear stress that constitutes the frictional drag is equivalent to $\tau_0 \sin\theta$ for any arbitrary point on the surface of the sphere.

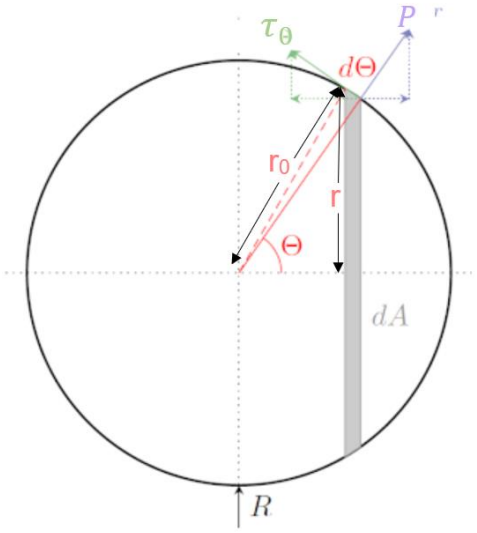

Figure 2.8 *Friction Drag acting on a sphere ("Deriving Stokes' Law in a Simple Way.")*

Using figure 2.7 on the left

$$\sin\theta = \frac{r}{r_0} \qquad (26)$$

Substituting τ_0 and $\sin\theta$

$$\tau_0 \sin\theta = \frac{-4\eta v}{(R-r)}\frac{r}{r_0} \qquad (27)$$

To determine the frictional drag, equation 27 is integrated with respect to the differential area dA:

$$F_{(wall)friction} = \int_0^A \tau_0 \sin\theta \; dA = \int_0^A \frac{-4\eta v}{(R-r)}\frac{r}{r_0} dA \qquad (28)$$

Substituting differential area as $dA = r\,dr\,d\emptyset$ described by cylindrical coordinates

$$F_{(wall)friction} = \frac{-4\eta v}{r_0}\int_0^{2\pi}\int_0^{r_0}\frac{r^2}{R-r}\,dr\,d\emptyset \qquad (29)$$

To solve the inner integral $\int_0^{r_0}\frac{r^2}{R-r}\,dr$, in equation 29, integration by substitution is used ***(Appendix B)***.

$$F_{(wall)friction} = \frac{-8\pi\eta v}{r_0}\left[R^2\,ln\left|\frac{R}{R-r_0}\right| - \frac{r_0^2-2Rr_0}{2} - 2Rr_0\right] \qquad (30)$$

The negative sign will be ignored as only the magnitude is required.

$$\therefore F_{(wall)friction} = \frac{8\pi\eta v}{r_0}\left[R^2\,ln\left|\frac{R}{R-r_0}\right| - \frac{r_0^2-2Rr_0}{2} - 2Rr_0\right] \qquad (31)$$

Dividing the terms in the bracket both by r_0^2 of equation 31 gives

$$F_{(wall)friction} = 8\pi\eta v r_0\left[\frac{R^2}{r_0^2}ln\left|\frac{R}{R-r_0}\right| - \frac{r_0^2-2Rr_0}{2r_0^2} - \frac{2R}{r_0}\right] = 8\pi\eta v r_0\left[\frac{R^2}{r_0^2}ln\left|\frac{R}{R-r_0}\right| - \frac{R}{r_0} - \frac{1}{2}\right] \qquad (32)$$

The total drag force exerted by wall is equal to the sum of wall friction and drag in an unbounded medium (which equals $6\pi\mu r_0 v$).

$$F_{(Drag)Total} = 8\pi\eta v r_0\left[\frac{R^2}{r_0^2}ln\left|\frac{R}{R-r_0}\right| - \frac{R}{r_0} - \frac{1}{2}\right] + 6\pi\mu r_0 v \qquad (33)$$

$$F_{(Drag)Total} = 2\pi\eta v r_0\left[\frac{4R^2}{r_0^2}ln\left|\frac{R}{R-r_0}\right| - \frac{4R}{r_0} + 1\right] \qquad (34)$$

The relative drag force (K_{Drag}) exerted by the wall effect is calculated by the ratio of drag force experienced inside a bounded medium (F_B) to an unbounded medium ($F_\infty = 6\pi\mu r_0 v$). $F_B = F_{(Drag)Total}$.

$$K_{Drag} = \frac{F_B}{F_\infty} = \frac{2\pi\eta v r_0\left[\frac{4R^2}{r_0^2}ln\left|\frac{R}{R-r_0}\right| - \frac{4R}{r_0} + 1\right]}{6\pi\mu r_0 v} = \frac{1}{3}\left(\frac{4R^2}{r_0^2}ln\left|\frac{R}{R-r_0}\right| - \frac{4R}{r_0} + 1\right) \qquad (35)$$

Expressing this equation in terms of the relative radius ($D = \frac{r_0}{R}$) where r_0 is the sphere radius and R is the tube radius, $\frac{r_0}{R}$ will be substituted by D.

The theoretical value is modelled using:

$$K_{Drag} = \frac{F_B}{F_\infty} = \frac{4}{3D^2} ln \left|\frac{1}{1-D}\right| - \frac{4}{3D} + \frac{1}{3} \qquad (36)$$

The relative drag force is independent of the ball radius or the tube radius but rather dependent on the ratio between the two which is defined by the variable D.

Equation 36 will be used to calculate the theoretical value for the relative drag force which will be used to compare the experimentally determined value to propagate the percentage error.

f. Accuracy of the Theoretical Model

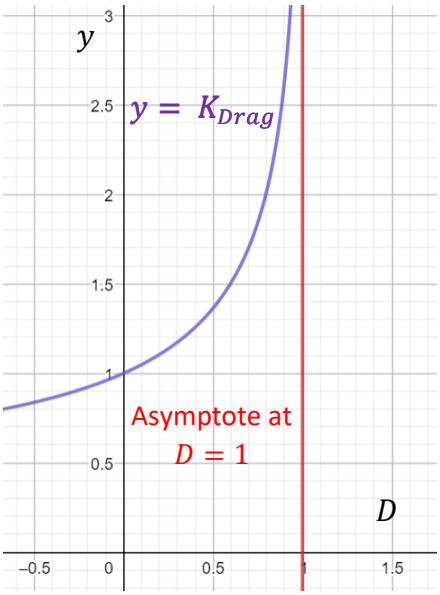

Figure 2.9 *Relative Drag vs. Relative Radius Graph – Theoretical Model on Geogebra (Candidate, 2021)*

Examining the theoretical model, the relative radius D approaches 0, relative drag force equals 1 as well which is self-explanatory because $F_B = F_\infty$ and $K_{Drag} = \frac{F_\infty}{F_\infty} = 1$.

At $D = 1$, the relative drag approaches infinite as indicated by the vertical asymptote in red in the figure 2.9 which makes sense because the velocity gradient will also approach infinite.

V. VARIABLES

a. Independent Variable

The independent variable in this exploration is the relative radius of the bounded medium (the ratio of the radius of the ball bearing to the radius of the cylindrical tube). The relative radius (unitless dimension) will be calculated by the equation $D = \frac{r_0}{R}$, where D represent the relative radius, r_0 is radius of the ball bearing and R is tube radius. The radius of the ball bearing and the glass tube will be measured using a vernier calliper (± 0.01 cm). A range of 7 different increments of relative radius (table 1) are used to collect sufficient data. The percentage uncertainty is calculated using the formula $\Delta = \frac{Absolute\ Uncertainty}{Actual\ Reading} \times 100$. The absolute uncertainty in the relative radius (D) is calculated by $\frac{\%\ Uncertainty\ in\ the\ D}{100} * Actual\ Value$, where the % uncertainty in relative radius is equivalent to the sum of % uncertainty in the tube radius and the ball radius.

Table 1 Calculating the relative radii & uncertainties for the ball bearings

Tube Radius (R/cm) = 1.25 ± 0.01 cm

% Uncertainty in Tube Radius (ΔR) = 0.8 %

Ball Radius (r_0/cm) ($\Delta r_0 = \pm 0.01$ cm)	% Uncertainty in Ball Radius (Δr_0)	**Relative Radius** $\boldsymbol{D = \frac{r_0}{R}}$	Absolute Uncertainty in Relative Radius (ΔD)*
0.25	4.00	**0.20**	0.0096
0.38	2.63	**0.30**	0.0104
0.50	2.00	**0.40**	0.0112
0.60	1.67	**0.48**	0.0118
0.88	1.14	**0.70**	0.0136
0.95	1.05	**0.76**	0.0141
1.10	0.91	**0.88**	0.0150

**Since the absolute uncertainty was too small to be shown, 4 significant figures are quoted.*

b. Dependent Variable (DV)

- The raw dependent variable is the terminal velocity (v_t/ms^{-1}) of the ball bearing, determined using video analysis on Logger Pro.
- The processed dependent variable within this exploration is the relative drag ($K_{Drag} = \frac{F_B}{F_\infty}$) which is the ratio of drag force experienced inside a bounded medium (F_B) to that experienced inside an unbounded medium (F_∞), which is a unitless quantity.

According to Stokes law ($F_D = 6\pi r_0 \eta v$) because $F_{Drag} \propto \eta$, then $\frac{F_B}{F_\infty} = \frac{\eta}{\eta_\infty}$ where η is the viscosity of glycerol in a bounded medium, and η_∞ is the viscosity of glycerol in an unbounded medium. This will be determined using equation 19: $\boldsymbol{\eta = \frac{2{r_0}^2 g}{9 v_t}\left(p_{sphere} - p_{fluid}\right)}$ where the terminal velocity inside the bounded medium $(\boldsymbol{v_{t,B}})$ and the unbounded medium $(\boldsymbol{v_{t,\infty}})$ will be used to determine the viscosity in the respective mediums.

c. Controlled Variables

Table 2 Justification and method of control for controlled variables

Variable	Why is it controlled?	How can it be controlled?
Fluid Viscosity	Each fluid has a different density and flow regime, and this will affect the overall amount of drag experienced because the drag force is directly proportional to the fluid viscosity therefore if the type of liquid varies then the drag force will fluctuate too.	This is controlled by utilizing the same Newtonian fluid, Glycerol. The initial viscosity of the fluid will be determined using a viscosimeter.
The density of Sphere and the fluid	The drag force acting on a spherical body is dependent upon the density of the sphere and the fluid. If the density of the ball bearing or the fluid varies it will cause the terminal velocity to vary between each increment causing inconsistency.	This is controlled by using a ball bearing of uniform density from the same manufacturer and material and the same Newtonian fluid (Glycerol) will be used from the same sample.
Fluid Temperature (°C)	The temperature of the fluid affects the viscosity and the density of the fluid this will cause the buoyant and cause variations in the relative drag and produce inaccurate readings.	This is controlled by conducting the practical in a controlled environment with ambient temperature (25 °C) by

		verifying the temperature using a temperature probe.
Rotational Dynamics	Rotational forces acting on the ball bearing can influence the angular momentum and velocity of the sphere and therefore the resultant drag force experienced on the surface of the body will vary.	This can be controlled by the using an electromagnet as a hold and released mechanism to prevent any rotational energy given to the ball bearing when dropping it by hand.
Drop height of the ball bearing	The drop height of the ball bearing will cause the frictional drag to vary because a greater distance more shear forces will arise.	This is controlled by keeping the drop height constant 50 cm, which will be measured using a meter stick and will be marked on to the cylindrical tube.

Other Consideration (End effect) – The base of the cylindrical tube also exerts an end effect which varies depending on the proximity of the base relative to the ball, therefore if the distance to the end (for ball tracking) is lesser then the base this end effect will be negligible.

VI. EXPERIMENT

a. Apparatus

Table 3 Apparatus Requirements

Equipment	**Quantity**
Vernier Caliper (± 0.01 cm)	x1
Ball Bearings (7 of different radii)	x1 each
Glycerol	500 cm^3
Temperature Probe (± 0.5 °C)	x1
Clamp Stand	x2
Cylindrical Tube (radius 1.25 cm)	x5
Permanent Magnets	x2
Iron Hex Head Bolt	x1
Coil of Wire	x1
Crocodile Clips	x2
9-Volt Battery	x1
Video Camera	x1
Logger Pro Software	x1
Bubble Wrap	x1 roll

b. Experimental Set-up

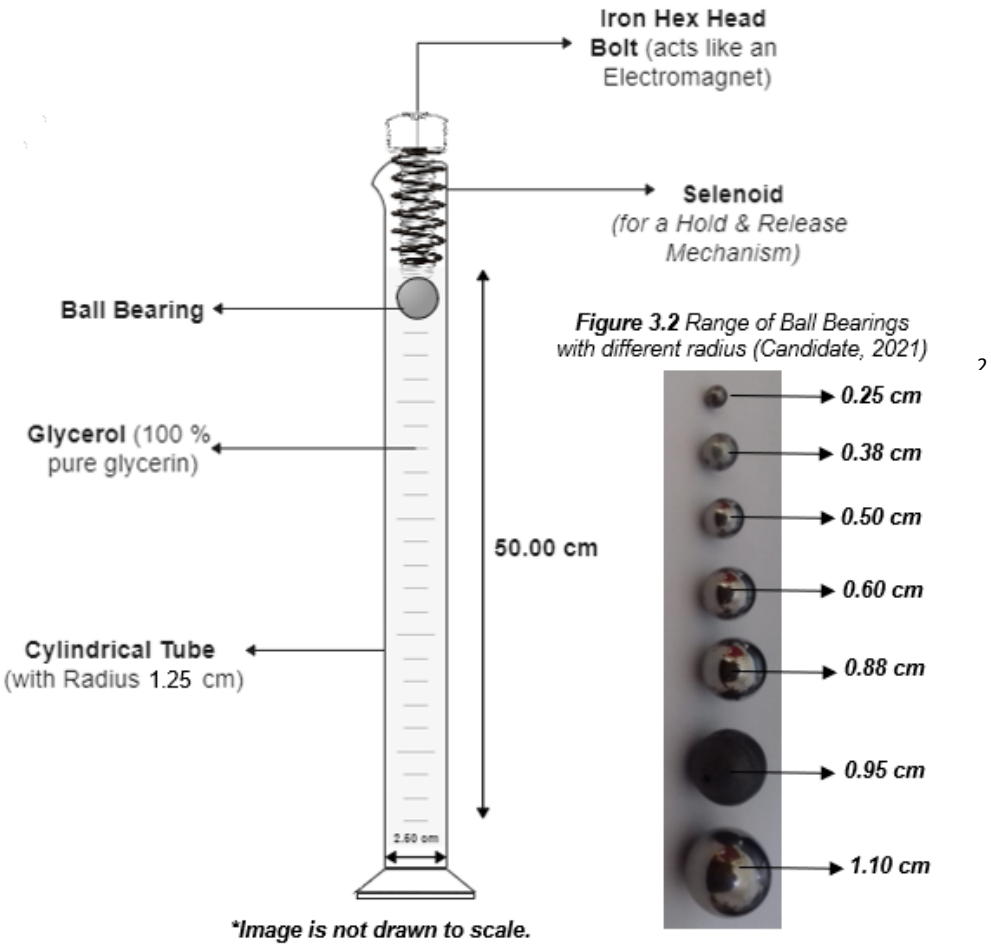

Figure 3.1 *Sketch for the Set-Up of the Apparatus (Candidate, 2021)*

c. Assumptions

i. The flow regime is strictly laminar.

ii. No rotational forces are acting on the ball bearing.

iii. The ball bearing experiences the wall effect due to frictional drag only.

iv. The velocity gradient is to equal zero in an unbounded medium (acceleration of fluid is spread for an infinite distance from the ball bearing).

d. Methodology

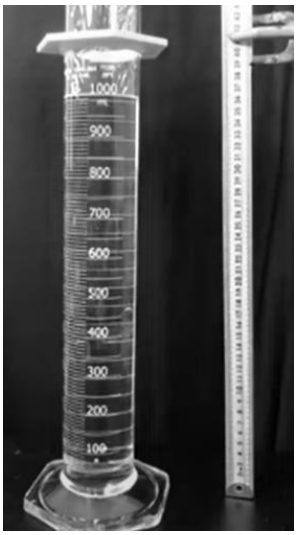

Figure 3.3 *Experimental Set-up (Candidate, 2021)*

Safety considerations and construction of a release-mechanism is addressed in Appendix C. A cylindrical tube was cleaned with distilled water and place bubble wrap was placed at the bottom of the tube to increase the duration of time where ball bearing imparts a force on base. The tube was filled with glycerol and placed the ball bearing (radius 0.25 cm) below the electromagnet over the open end of the cylindrical tube (refer to experimental set-up).

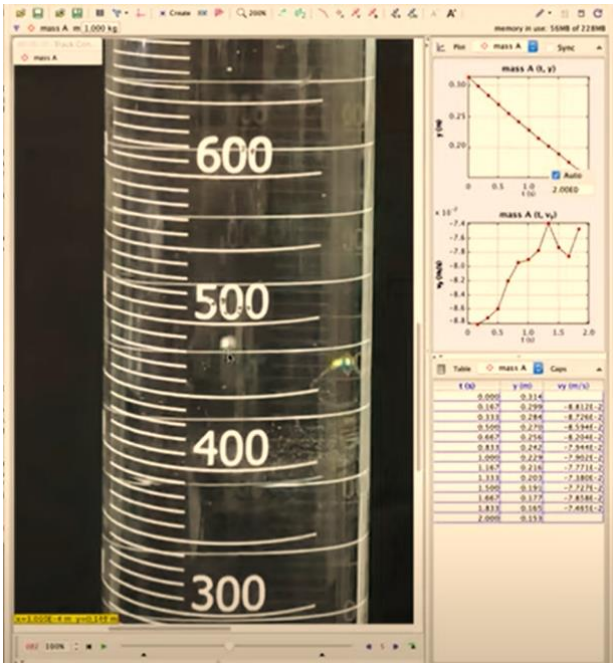

Figure 3.4 *Ball Tracking on Logger Pro (Candidate, 2021)*

The video camera was placed one meter away from the set-up and tracked the motion of the ball within 25 frames per second. Terminal velocity was extrapolated from the logger pro tracking software and allowed the calculation of the viscosity for the ball bearing in the bounded medium and the relative drag force ($K_{Drag} = \frac{F_B}{F_\infty}$).

Steps 1-9 were repeated for 4 more trials and step 1-10 were repeated for all other range of relative radii.

VII. DATA COLLECTION

The terminal velocity for each trial was determined by an extrapolating the strong linear portion of the (velocity-time) graph where the gradient was zero and the velocity was maximum.

a. Raw Data – Relative radius of the bounded medium vs. the terminal velocity

Table 4 Raw Data Collection of Terminal Velocity in a Bounded Medium

Relative Radius $(D = \frac{r_0}{R})$	**Terminal Velocity of the Ball Bearing** $(v_{t,B}\ /ms^{-1})$				
	Trial 1	**Trial 2**	**Trial 3**	**Trial 4**	**Trial 5**
0.20	0.064322	0.059834	0.063121	0.058842	0.063036
0.30	0.134572	0.126253	0.123212	0.130123	0.125580
0.40	0.194076	0.190452	0.185945	0.187584	0.192483
0.48	0.242855	0.252319	0.256254	0.259543	0.280694
0.70	0.425508	0.410583	0.395428	0.400178	0.412598
0.76	0.392958	0.401295	0.386849	0.396284	0.379274
0.88	0.439528	0.421237	0.428693	0.419285	0.439282

The mean terminal velocity is calculated by

$$Mean\left(\boldsymbol{v_{t,B}}\right) = \frac{\sum_{i=1}^{5} \boldsymbol{Trial\ x}}{\mathbf{5}} \qquad (37)$$

b. Processed Data

i. Propagating the percentage uncertainty in Terminal Velocity

Since the terminal velocity is quoted to 6 significant figures on Logger pro which is extremely precise, the absolute experimental uncertainty in terminal velocity is propagated using an alternative method:

$$Absolute\ Experimental\ Uncertainty = \frac{\max - min}{2} \quad (38)$$

$$Percentage\ Experimental\ Uncertainty = \frac{Absolute\ Uncertainty}{Mean\ Terminal\ Velocity} \times 100 \quad (39)$$

Table 5 Calculating Uncertainty in Terminal Velocity

Relative Radius ($D = \frac{r_0}{R}$)	**Mean Terminal Velocity in a** Bounded Medium **($v_{t,B}\ /ms^{-1}$)**	**Max Value of $v_{t,B}$**	**Min Value of $v_{t,B}$**	**Absolute Experimental Uncertainty in $v_{t,B}$**	**Percentage Experimental Uncertainty in $v_{t,B}$**
0.20	0.061831	0.064322	0.058842	0.002740	4.431
0.30	0.127948	0.134572	0.123212	0.005680	4.439
0.40	0.190108	0.194076	0.185945	0.004066	2.139
0.48	0.258333	0.280694	0.242855	0.018920	7.324
0.70	0.408859	0.425508	0.395428	0.015040	3.679
0.76	0.391332	0.401295	0.379274	0.011011	2.814
0.88	0.429605	0.439528	0.419285	0.010122	2.356

ii. Processing the Relative Drag Force

The terminal velocity was used to calculate the relative drag force (K_{Drag}) acting on the ball bearing due to the wall effect.

Since $F_{Drag} \propto \eta$ because of stokes law ($F_D = 6\pi r_0 \eta v$), then $K_{Drag} = \frac{F_B}{F_\infty} = \frac{\eta}{\eta_\infty}$ where η is the viscosity of glycerol in a bounded medium, and η_∞ is the viscosity of glycerol in an unbounded medium.

This will be determined using equation 10 where the terminal velocity inside the bounded medium ($\boldsymbol{v_{t,B}}$) and the unbounded medium ($\boldsymbol{v_{t,\infty}}$) will be used to determine the viscosity in the respective mediums. The viscosity of pure glycerin is 1.412 Pa·s in an unbounded medium. The ratio between the viscosity in bounded and unbounded medium ($K_{Drag} = \frac{F_B}{F_\infty} = \frac{\eta}{\eta_\infty}$) will be used to calculate the relative drag force (see table 6).

The uncertainty in the experimental drag is the same as the uncertainty in mean terminal velocity because η_∞ is a constant literature value with no uncertainty. Thus, the major source of uncertainty is the experimental uncertainty of the terminal velocity.

Table 6 Calculating Uncertainty in Terminal Velocity				
Relative Radius ($D = \frac{r_0}{R}$)	**Mean Viscosity (η)** in a Bounded Medium (Pa·s)	**Mean Viscosity (η_∞)** in an Unbounded Medium (Pa·s)	**Experimental Relative Drag** (K_{Drag})	**Percentage Experimental Uncertainty**
0.20	1.45436	1.412	1.03	4.431
0.30	1.62380	1.412	1.15	4.439
0.40	1.89208	1.412	1.34	2.139
0.48	2.00504	1.412	1.42	7.324
0.70	2.72516	1.412	1.93	3.679
0.76	3.31820	1.412	2.35	2.814
0.88	4.05244	1.412	2.87	2.356
Average Percentage Uncertainty				3.883

iii. Propagating Theoretical Values of Relative Drag

Using the formula derived in equation 36, theoretical values of the relative drag force are determined.

$$K_{Drag} = \frac{F_B}{F_\infty} = \frac{4}{3D^2} ln \left|\frac{1}{1-D}\right| - \frac{4}{3D} + \frac{1}{3}$$

Table 7 Theoretical Values of the Relative Drag Force

Relative Radius ($D = \frac{r_0}{R}$)	Theoretical ($K_{Drag\ (Theor)}$) Model
0.20	1.10
0.30	1.17
0.40	1.25
0.48	1.33
0.70	1.70
0.76	1.87
0.88	2.46

iv. Propagating Literature Values of Relative Drag

The terminal velocity is used to calculate the relative drag force acting on ball bearing due to the wall effect.

The literature values are propagated using the data reported by Atiade. The figure shows the effect of the relative radius on the wall factor expressed by f_w. In the graph below d_f/D_r represents the relative radius, while wall factor, f_w, is used to quantify the degree of influence of the wall effect on the terminal velocity of particle in consideration. The wall factor $f_w = \frac{v_{t,B}}{v_{t,\infty}}$ is the ratio of terminal velocity inside a bounded medium ($v_{t,B}$) to an unbounded medium ($v_{t,\infty}$).

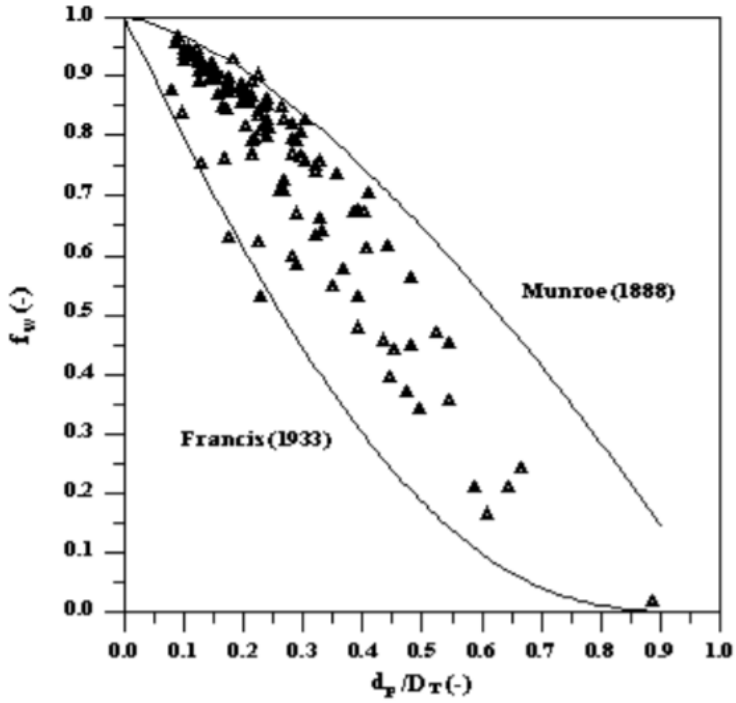

Figure 4.1 *Literature Value of the Wall Factor at different relative radii (Atiade)*

The literature value of the relative drag force equals

$$K_{Drag} = \frac{F_B}{F_\infty} = \frac{\eta}{\eta_\infty} = \frac{v_{t,\infty}}{v_{t,B}} = \frac{1}{f_w}$$

The inverse-relationship exists because viscosity is inversely related to the terminal velocity ($\eta = \frac{2{r_0}^2 g}{9v_t}(p_{sphere} - p_{fluid})$). Since force is directly proportional to viscosity according to stokes law the ratio of the drag force must be inversely related to the wall factor.

Secondary Resource Evaluation: Using the data from Munroe's curve (1888) is interpolated to determine the literature value of the drag force. This secondary data is valuable because it will determine the accuracy of the results obtained but it is also limited by the date produced (the data reported is more than 30 years old).

Table 8 – Literature value of the Relative Drag from Munroe (1888)

Relative Radius $(D = \frac{r_0}{R})$	**Wall Factor (f_w) Munroe (1888)**	**Literature Value of Relative Drag** $(K_{Drag} = \frac{1}{f_w})$
0.20	0.93	1.08
0.30	0.85	1.18
0.40	0.75	1.33
0.48	0.67	1.49
0.70	0.41	2.44
0.76	0.34	2.94
0.88	0.23	4.35

c. Propagating the Percentage Error

Percentage error in the relative drag value is determined using:

$$\%\ Error = \left|\frac{Expected\ Value - Experimental\ Value}{Expected\ Value}\right| \times 100$$

The experimental value is compared to expected value (both theoretical and literature) to determine the accuracy of the results obtained.

Table 9 – Percentage Error using Theoretical and Literature Model

Relative Radius $(D = \frac{r_0}{R})$	**Value of the Relative Drag** $(K_{Drag} = \frac{F_B}{F_\infty})$				
	Experimentally Determined $(K_{Drag\ (Exp)})$	Theoretical $(K_{Drag\ (Theor)})$	% error relative to theoretical	Literature $(K_{Drag\ (Lit)})$	% error relative to literature
0.20	1.03	1.10	6.36 %	1.08	4.63 %
0.30	1.15	1.17	1.71 %	1.18	2.54 %
0.40	1.34	1.25	7.20 %	1.33	0.75 %
0.48	1.42	1.33	6.77 %	1.49	4.70 %
0.70	1.93	1.70	13.53 %	2.44	20.90 %
0.76	2.35	1.87	25.67 %	2.94	20.07 %
0.88	2.87	2.46	16.67 %	4.35	34.02 %
Average Percentage Error			11.13 %		12.52 %

VIII. GRAPHICAL ANALYSIS

In graph 4.2, horizontal error bars represent the equipment uncertainty of the vernier caliper that measure the radius of the tube and the ball. The vertical error bars reflect the experimental uncertainties in the relative drag force which was propagated by finding the experimental uncertainty in the mean terminal velocity. There exists an exponential fit between the relative radius of the bounded medium and the relative drag force.

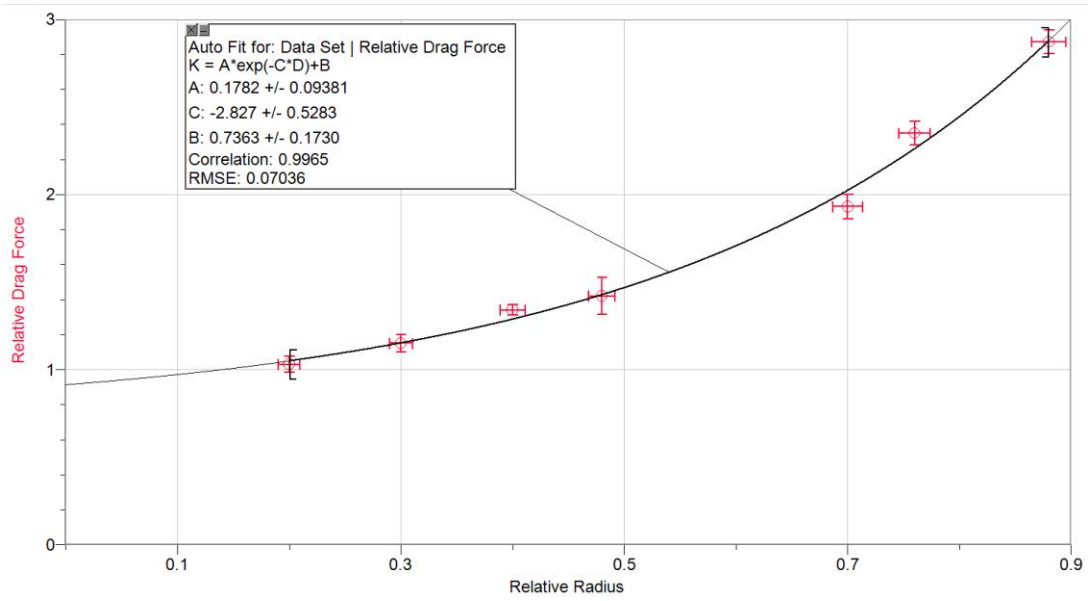

Figure 4.2 *Scatter Plot of Relative Radius vs. Relative Drag Force on LoggerPro (Candidate, 2021)*

The diagram below shows a comparison of experimental values with the literature and the theoretical model.

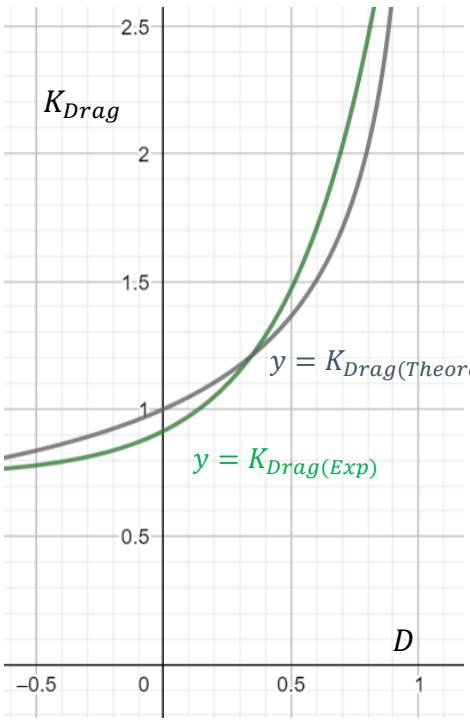

Figure 4.3 *Graph Theoretical Vs. Experimental Data (Candidate, 2021)*

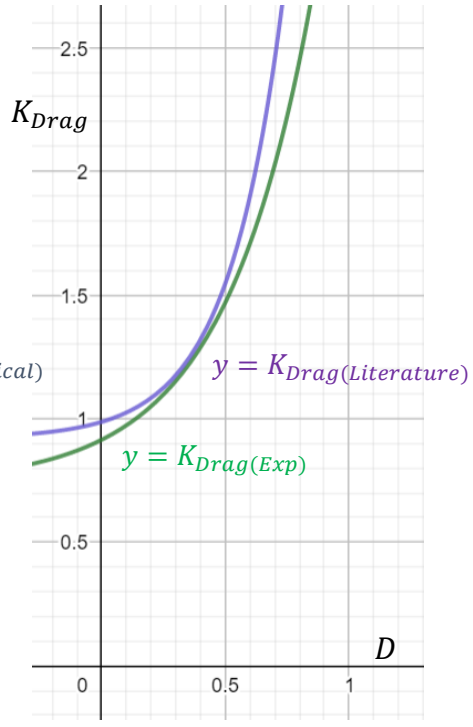

Figure 4.4 *Graph Literature Vs. Experimental Data (Candidate, 2021)*

The experimental data is extremely close to the literature and theoretical model however the drag force diverge off at large relative radii presumably because of the inaccuracies of the assumptions used to derive these models. In the first graph, coefficient of determination (R^2) is extremely close to 1 (precisely being 0.9965) which means that the strength of association between the relative radius and the relative drag force is extremely strong (as predicted by the theoretical model). It also conforms to the idea that the relative drag force is not directly dependent upon the radius of tube or the radius of the ball bearing but rather on the ratio between the two.

IX. METHOD EVALUATION

All plausible limitations are addressed below:

Table 10 Limitations/Evaluation of the Method

Limitation	Impact of Error	How to reduce this?
Number of trials conducted	Only 5 trials were conducted to calculate the mean of the terminal velocity. Although, this is sufficient, a greater number of trials would have allowed more reliable data to be obtained with smaller percentage uncertainty.	This can be improved by increasing the number of trials from 5 to 10 which will minimize the random error.
Increments of IV	Only 7 increments of relative radius were taken, however a greater range of IVs would allow sufficient and relevant data to be collected and a reliable trend and relationship can be drawn.	This can be improved by increasing the range of IVs from 7 to 10 by using additional ball bearings of different width.
Assumption	The change in pressure drag was assumed to be negligible with change in relative radius. However, it is important to consider this change because the relative radius does impose a change in pressure with respect to the proximity of the wall.	This can be improved by considering the pressure drag whilst deriving the total drag force.

X. CONCLUSION

Examining the results of the experimental and the theoretical model, the research question investigating “How does the relative radii of a ball bearing affect the relative drag force experienced within a Newtonian fluid?” can be effectively answered.

As the relative radius increases, the relative drag force inside a bounded medium increases exponentially as well. The experimental data has a strong connection and accurately resemble the theoretical models and literature model, despite the slight deviations where the relative radius approaches the value of 1. This substantiates that accuracy of the results obtained as observed by the low average percentage error of 11.13 % (relative to the theoretical model) and 12.52 % (relative to the literature model). This difference relative to the literature and theoretical model can be attributed to the assumptions (of the pressure drag and no rotational forces) made whilst deriving the relationship. The graph shows evidence of small systematic and random errors. There are also deviations because of the adhesive forces between the fluid and boundary layer and the cohesive forces of the fluid. It is also observed that at large values of r_0, the experimental values deviate from the theoretical and literature model which is because of a direct contact (radius-dependent phenomenon) and a cause for a high percentage error. Regardless, the results obtained are extremely precise as observed by the extremely low average percentage uncertainty of 3.883 % and a coefficient of determination of 0.9965. This low percentage uncertainty is attributable to the

precise equipment utilizing and the accurate video analysis using logger pro. Overall, the results obtain can be described as precise and accurate.

To **extend** the scope of this exploration the wall effect for non-spherical objects can be examined. Conducting the same study, but for non-spherical objects like cones and prisms and multiple objects can produce more meaningful results for examining how different shapes submerges inside single channels can impact the drag coefficient and the relative drag force experienced by the wall effect which can be employed in the food industries and modelling the wall effect for the motion of cells and bioengineering devices inside blood vessels.

Works Cited

Ahmed, Houari. 2012 *Eur. J. Phys*. 33 947.

Ataíde, C. H., et al. "Wall Effects on the Terminal Velocity of Spherical Particles in Newtonian and Non-Newtonian Fluids." *Brazilian Journal of Chemical Engineering*, Brazilian Society of Chemical Engineering, 1 Dec. 1999, www.scielo.br/j/bjce/a/BmBTmqdF9Qggz6ZZxj4kNNb/?lang=en. Accessed 20th July 2021.

"Deriving Stokes' Law in a Simple Way." *Physics Stack Exchange*, 1 Sept. 1968, physics.stackexchange.com/questions/537455/deriving-stokes-law-f-v-6-pi-eta-rv-in-a-simple-way. Accessed 24th July 2021.

Hall, Nancy. "Navier-Stokes Equations." *NASA*, NASA, www.grc.nasa.gov/www/k-12/airplane/nseqs.html. Accessed 23rd Aug. 2021.

"How to Make an Electromagnet." *YouTube*, Science Buddies, 12 Oct. 2016, youtu.be/Wm9_DqQKmd0. Accessed 23rd July 2021.

Nakayama, Yasuki, and Robert F. Boucher. *Introduction to Fluid Mechanics*. Butterworth-Heinemann, 2002.

Nave, Carl Rod. "Fluid Resistence." *Air Friction*, hyperphysics.phy-astr.gsu.edu/hbase/airfri.html. Accessed 28th Aug. 2021.

Ramsey, Mark S. "Pressure Drop Calculations." *Practical Wellbore Hydraulics and Hole Cleaning*, Gulf Professional Publishing, 8 Feb. 2019, www.sciencedirect.com/science/article/pii/B9780128170885000058. Accessed 25 July 2021.

Samantaray, Saroj Kumar, et al. "A Numerical Study of the Wall Effects for Newtonian Fluid Flow over a Cone." *Engineering Science and Technology, an International*

Journal, Elsevier, 9 Jan. 2018, www.sciencedirect.com/science/article/pii/S2215098617306717#f0010. Accessed 21st July 2021.

"Proof of Stokes Law of Viscosity Using Reynolds Law." *Young Scientists Journal*, 29 Mar. 2021, ysjournal.com/proof-of-stokes-law-of-viscosity-using-reynolds-law/. Accessed 23rd July 2021.

XI. APPENDICIES

Appendix A: Stokes Law

The two types of forces that act inside a fluid are frictional drag and pressure drag. The pressure drag (due to the pressure differences arising from the body shape and flow separation) acts perpendicularly to the surface of the body; whilst, the frictional drag (due to the friction between the layers of the fluid and the body and the boundary layer properties) acts tangentially to the surface of the object.

$$F_{Total\ Drag} = F_{friction} + F_{pressure} \quad (8)$$

The drag force at any position on a small element is expressed as:

$$dD = \tau_0\, dA \sin\theta + P\, dA \cos\theta \quad (9)$$

where P is the pressure, τ_0 is the viscous shear stress and dA is the differential area (see figure 2.4) at that point.

Since forces are only being considered at tiny surfaces, only the cylindrical segment needs to be taken into consideration whose area is given by the radius of the circle expressed as $R \sin\theta$ and the height equivalent to the differential arc length denoted by $R\, d\theta$. Therefore the differential area is the product of the circle's circumference and height, which can be expressed by:

$$dA = \underbrace{2\pi(R\sin\theta)}_{\text{Circumference}}\ \underbrace{R\, d\theta}_{\text{Height}} = 2\pi R^2 \sin\theta\, d\theta \quad (10)$$

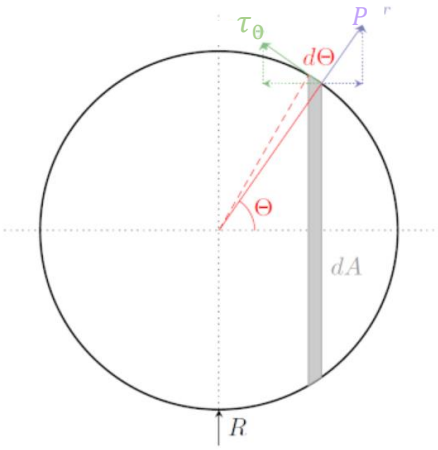

In order to evaluate the total drag on a body, the sum of all the shear stresses (tiny forces acting on each position) needs to be taken into account using the integration of the pressure and friction drag.

Figure 2.4 *Pressure & Friction Drag acting on a sphere ("Deriving Stokes' Law in a Simple Way.")*

$$F_{Total\ Drag} = \int dD = \underbrace{\int_0^\pi \tau_0 \sin\theta\, dA}_{\text{Friction Drag } (D_F)} + \underbrace{\int_0^\pi P \cos\theta\, dA}_{\text{Pressure Drag } (D_P)} \qquad (11)$$

Substituting the value of dA (in equation 10) into equation 11 ("Deriving Stokes' Law in a Simple Way."):

$$F_{Total\ Drag} = 2\pi R^2\left[\int_0^\pi \tau_0 sin^2\theta\, d\theta + \int_0^\pi P \sin\theta \cos\theta\, d\theta\right] \qquad (12)$$

In stokes law, integrating equation 12 yields:

$$D_F = 4\pi r_0 \eta v \quad \& \quad D_P = 2\pi r_0 \eta v \qquad (13\ \&\ 14)$$

$$F_{Total\ Drag} = 4\pi r_0 \eta v + 2\pi r_0 \eta v = 6\pi r_0 \eta v \qquad (15)$$

where r_0 is the radius of the spherical object, η is the viscosity of the fluid and v is the velocity of the sphere which *is the definition of stokes law.*

Appendix B: Integration by Substitution

To solve the inner integral $\int_0^{r_0} \frac{r^2}{R-r} dr$, in equation 29, integration by substitution is used.

Substitution: Let $u = R - r$

Since R is a constant, $\frac{du}{dr} = -1$. Thus $dr = -du$.

Using the substitution above inner integral now simplifies to

$$\int_0^{r_0} \frac{r^2}{R-r} dr = -\int_0^{r_0} \frac{(R-u)^2}{u} du = -\int_0^{r_0} \left(\frac{R^2}{u} - 2R + u\right) du = -\left[R^2\, ln|u| + \frac{u^2}{2} - 2Ru\right]_0^{r_0} \quad (1)$$

Resubstituting $u = R - r$, into the integral above gives

$$\int_0^{r_0} \frac{r^2}{R-r} dr = -\left[R^2\, ln|R-r| + \frac{(R-r)^2}{2} - 2R(R-r)\right]_0^{r_0} \quad (2)$$

The equation above simplifies to

$$-R^2\, ln|R-r_0| - \frac{(R-r_0)^2}{2} + 2R(R-r_0) + R^2\, ln|R| + \frac{R^2}{2} - 2R^2 \quad (3)$$

Using property of logarithms and collecting like terms, equation 3 equals

$$\int_0^{r_0} \frac{r^2}{R-r} dr = R^2\, ln\left|\frac{R}{R-r_0}\right| - \frac{r_0^2 - 2Rr_0}{2} - 2Rr_0 \quad (4)$$

This inner integral can now be resubstituted into the outer integral

$$\int_0^{2\pi}\int_0^{r_0} \frac{r^2}{R-r} dr\, d\emptyset = \int_0^{2\pi} \left[R^2\, ln\left|\frac{R}{R-r_0}\right| - \frac{r_0^2 - 2Rr_0}{2} - 2Rr_0\right] d\emptyset \quad (5)$$

Since no terms containing ∅ are present, the integral above can be resolved by multiplying the integrand with $[\emptyset]_0^{2\pi}$ which is 2π.

Appendix C: Methodology

Safety Considerations

a. **Glassware –** All glassware apparatus are fragile (can shatter into small pieces) and should be handled with care. Avoid touching shattered pieces with bare hands.
b. **Ball Bearings –** Large ball bearings are heavy and can cause damage if dropped from a height; therefore avoid keeping them unequipped near the edge of tables.
c. **Diagonal Cutting Plier (Wire Cutter) –** It is sharp and can damage skin so carefully cut the copper wire keeping any vulnerable items away from the blade.

Making an Electromagnet *(for a Hold & Release Mechanism)* ("How to Make an Electromagnet.")

i. Wrap the coated copper wire around the Iron Hex Head Bolt to produce a 100 coils.
ii. Cut the remaining wire using a diagonal cutting plier, leaving a 10 cm excess on both sides of the electromagnet.
iii. Using the sand paper, sand the edges of the copper wire to remove the enamel coating.
iv. Connect both the crocodile clips with end to the copper wire and the other end to the terminals of the 9-volt battery.

v. Clamp the electromagnet (Iron Hex Bolt) 5 cm above the top of the cylindrical tube (measuring cylinder).

vi. Plug the battery into the socket and switch it on.